

Strain-induced changes of oxygen ordering in $\text{YBa}_2\text{Cu}_3\text{O}_{6+\delta}$ cupratesQ. P. Meng,^{1,2} David O. Welch,¹ and Y. Zhu^{1,*}¹Brookhaven National Laboratory, Upton, New York 11973, USA²School of Materials Science and Engineering, Shanghai Jiao Tong University, Shanghai 200030, China

(Received 30 October 2008; published 29 April 2009)

Local elastic strain may significantly alter oxygen ordering in superconducting cuprates due to the change in bond lengths and crystal symmetry, thus altering their superconducting properties. To explore this phenomenon, the Bragg-Williams and Bethe order-disorder theories were used in this study. We demonstrate that oxygen ordering may exist in locally strained regions at any finite temperature and that applied stresses change the overall order-disorder transition temperature. The states of order in oxygen-ordering domains near an edge dislocation and a twin tip in $\text{YBa}_2\text{Cu}_3\text{O}_{6+x}$ were calculated in both the low-temperature orthorhombic and high-temperature tetragonal. In the orthorhombic phase, both deviatoric and hydrostatic components of stress alter the degree of oxygen ordering at a given temperature and alter the superconducting transition temperature.

DOI: 10.1103/PhysRevB.79.134531

PACS number(s): 74.72.-h, 61.72.Mm

I. INTRODUCTION

The order-disorder phase transition has been studied for decades,¹⁻⁸ mostly in the case of simple alloys such as Cu-Au and Cu-Zn alloy. Recently, studies of cuprate oxides have revealed that the atomic and electronic structural properties of these compounds, including atomic, spin, and orbital orderings,⁹⁻¹⁵ are closely related to order-disorder phase transitions, which it is well known that oxygen ordering in the Cu-O plane of the high-temperature superconductor $\text{YBa}_2\text{Cu}_3\text{O}_{6+x}$ (YBCO) alters its superconducting transition temperature¹¹⁻¹³ and the interplay between atomic ordering, charge, and orbital ordering in colossal magnetoresistive manganites changes their magnetic and resistive properties.^{10,14,15}

In general, the theoretical tools used to study the order-disorder phase transition in oxides are still classical ones. For example, the mean-field approximation,¹⁶ quasi-chemical^{17,18} and cluster variation¹⁹ methods have been applied to oxygen ordering in YBCO. However, in these studies, except for the ordered atoms, atoms were assumed not to depart from their equilibrium positions, i.e.,

structural relaxation and elastic strain effects were not included. Therefore, these studies only considered the effects of temperature on the equilibrium locations of oxygen atoms in Cu-O planes and their effects on crystal symmetry. Figures 1(a)–1(c) illustrate this transition of oxygen filling of sites in the available sites in the Cu-O plane in YBCO, where A denotes an oxygen atom, B a vacancy, and C a copper atom. The C atoms are fixed at their equilibrium positions, while the A and B atoms can move between the α and β sites.

In the real situation, crystals are not ideal and homogeneous in their structure and thus the averaged crystal symmetry is often broken locally when atoms in the non-Cu-O planes in YBCO deviate from their equilibrium sites due to local stresses, crystal defects, and so on, as shown in Fig. 1(d). Then, the α and β sites of the Cu-O planes are not equivalent, so the order-disorder phase transition will change compared to its behavior in ideal homogeneous crystals.

The Bragg-Williams approximation is a common method employed to study the order-disorder phase transition in crystals because it yields simple formulae for free energy, degree of order, and temperature. The theory of Bethe, which is equivalent to the quasi-chemical-method, not only gener-

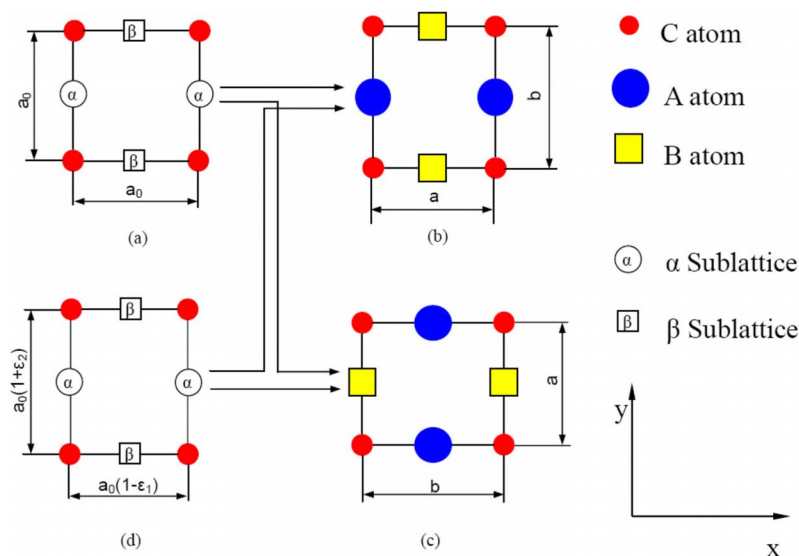


FIG. 1. (Color online) A schematic of a two-dimensional lattice changing from square to rectangle. (a) The original square lattice. [(b) and (c)] The rectangle lattice when A atoms occupy regularly on α sites and β sites, respectively (or vice versa for B atoms). (d) The original square lattice is strained. Unless otherwise noted, A usually refers to an oxygen ion, B to a vacant site, and C to a copper ion.

ates a more exact result than the Bragg-Williams approximation, because it takes into account short-range as well as long-range order, and also its theoretical derivation is easier to understand. In this study we used both the Bragg-Williams and Bethe theories to study the local strain-induced change of the state of oxygen ordering at thermodynamic equilibrium in YBCO cuprates containing nonhomogeneous elastic strain fields, arising for example from dislocations or twin-boundary tips. We then compare the results of the two theories and use them to explain some experimental observations.

II. THERMODYNAMIC THEORY

Easthope³ first introduced the factors λ and μ to account for the *a priori* probabilities of *A* and *B* atoms, respectively, occupying α and β sites. Because in his treatment these probabilities were equal, he could use one factor λ for the *A* atom, and one factor μ for the *B* atom. In simple binary alloys, this approach is always correct. Thus, looking at Figs. 1(a) and 1(d), if *C* atoms do not exist, the probabilities of *A* atoms occupying α and β sites are the same, as they are for *B* atoms. But if *C* atoms exist and deviate from their equilibrium position Fig. 1(d), the probabilities of *A* atoms occupying α and β sites differ. Therefore, we introduce the factors $\lambda_{A\alpha}$ and $\lambda_{A\beta}$ to account for the *a priori* probabilities of *A* atoms occupying α and β sites, and $\mu_{B\alpha}$ and $\mu_{B\beta}$ to *B* atoms. [In this study, *A* (see Fig. 1) will usually denote oxygen ions and *B* will denote vacant sites, unless noted otherwise, while *C* denotes Cu ions.]

According to the usual thermodynamic practice, $\lambda_{A\alpha} \propto \exp(-\frac{v_{A\alpha}}{k_B T})$, where $v_{A\alpha}$ is the energy change resulting when an *A* atom is placed on an α site, i.e., the “formation” energy of an *A* atom on an α site; $\lambda_{A\beta}$, $\mu_{B\alpha}$, and $\mu_{B\beta}$ have a similar relationship with $v_{A\beta}$, $v_{B\alpha}$, and $v_{B\beta}$. In the presence of an elastic strain field the interatomic separations of the neighboring atoms to the site where a particular oxygen atom is to be inserted are different from their values in strain-free crystals, and thus the single-site formation energies are dependent upon the state of elastic strain. In Secs. II A and II B, we use Bragg-Williams theory and Bethe’s theory to discuss the equilibrium degree of order in the presence of an elastic strain field.

A. Bragg-Williams theory

According to Bragg-Williams theory, when the internal energy of the system of ions and lattice sites consists of pairwise interactions and site specific potential energies, the energy of a microstate is given by

$$W = \sum_i (Q_{AA}^{(i)} v_{AA}^{(i)} + Q_{BB}^{(i)} v_{BB}^{(i)} + Q_{AB}^{(i)} v_{AB}^{(i)}) + (x_{A\alpha} v_{A\alpha} + x_{A\beta} v_{A\beta} + x_{B\alpha} v_{B\alpha} + x_{B\beta} v_{B\beta}), \quad (1)$$

where $Q_{AA}^{(i)}$, $Q_{BB}^{(i)}$, and $Q_{AB}^{(i)}$ are the number of *AA*, *BB*, and *AB* pairs, and $v_{AA}^{(i)}$, $v_{BB}^{(i)}$, and $v_{AB}^{(i)}$ are the respective pairwise interaction energies. The terms in the last parentheses are the single-site formation energies defined in the previous section. The superscript “(i)” represents the *i*th near neighbors. For

example, $Q_{AA}^{(1)}$ is the number of *AA* nearest pairs; $Q_{AA}^{(2)}$ is that of *AA* next-nearest pairs. $x_{A\alpha}$, $x_{A\beta}$, $x_{B\alpha}$, and $x_{B\beta}$ are the number of *A* atoms on α and β sites, and *B* atoms on α and β sites, respectively.

Bethe and Kirkwood’s method^{2,4} is used to define a long-range order parameter, *S*, which quantifies the degree of long-range order as follows:

$$S = \frac{x_{A\alpha} - x_{A\beta}}{N} = \frac{x_{B\beta} - x_{B\alpha}}{N}. \quad (2)$$

Note that the degree of long-range order is a single-site (not pair) probability and will be affected directly by elastic strain fields through the strain dependence of the single-site formation energies $v_{A\alpha}$, etc.

From $x_{A\alpha} + x_{A\beta} = 2cN$, $x_{B\beta} + x_{B\alpha} = 2(1-c)N$ (*N* is the number of *A* atoms or *B* atoms, and *c* is the concentration of *A* atoms), we get

$$x_{A\alpha} = \frac{N}{2}(2c + S), \quad (3a)$$

$$x_{A\beta} = \frac{N}{2}(2c - S), \quad (3b)$$

$$x_{B\alpha} = \frac{N}{2}[2(1-c) - S], \quad (3c)$$

$$x_{B\beta} = \frac{N}{2}[2(1-c) + S]. \quad (3d)$$

Considering only the interaction of nearest-neighbor and next-nearest-neighbor *A* and *B* atoms, the ensemble average of the interaction energy of the nearest neighbor and next-nearest neighbor of *AA*, *BB*, and *AB* pairs obtained using the Bragg-Williams (mean-field) approximation are given by

$$\langle W_{AA}^{(1)} \rangle = \langle Q_{AA}^{(1)} \rangle v_{AA}^{(1)} = \frac{1}{4} N z (4c^2 - S^2) v_{AA}^{(1)}, \quad (4a)$$

$$\langle W_{BB}^{(1)} \rangle = \langle Q_{BB}^{(1)} \rangle v_{BB}^{(1)} = \frac{1}{4} N z [4(1-c)^2 - S^2] v_{BB}^{(1)}, \quad (4b)$$

$$\langle W_{AB}^{(1)} \rangle = \langle Q_{AB}^{(1)} \rangle v_{AB}^{(1)} = \frac{1}{2} N z [4c(1-c) + S^2] v_{AB}^{(1)}, \quad (4c)$$

$$\langle W_{AA}^{(2)} \rangle = \langle Q_{AA}^{(2)} \rangle v_{AA}^{(2)} = \frac{1}{8} N z (4c^2 + S^2) v_{AA}^{(2)}, \quad (4d)$$

$$\langle W_{BB}^{(2)} \rangle = \langle Q_{BB}^{(2)} \rangle v_{BB}^{(2)} = \frac{1}{8} N z [4(1-c)^2 + S^2] v_{BB}^{(2)}, \quad (4e)$$

$$\langle W_{AB}^{(2)} \rangle = \langle Q_{AB}^{(2)} \rangle v_{AB}^{(2)} = \frac{1}{4} N z [4c(1-c) - S^2] v_{AB}^{(2)}, \quad (4f)$$

where $v_{AA}^{(2)}$ includes the interaction energy of an *AA* atomic pair across a middle atom and that without a middle atom. $v_{BB}^{(2)}$ and $v_{AB}^{(2)}$ are similar. Substituting Eqs. (3) and (4) into Eq.

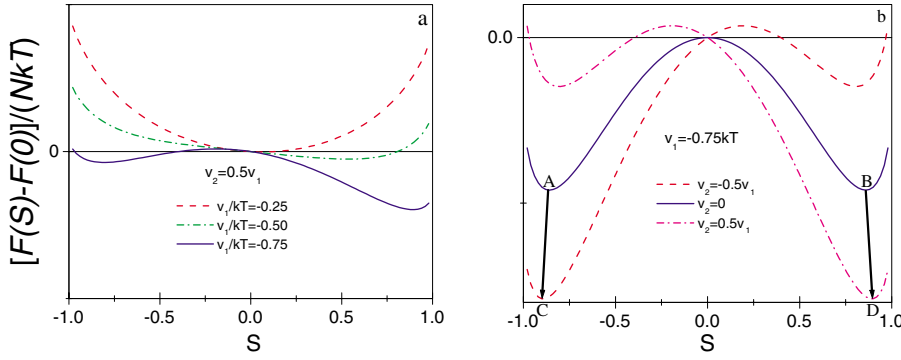


FIG. 2. (Color online) The free energy as function of long-range order parameter S according to the Bragg-Williams approximation [Eq. (6)] at various (a) temperatures T and (b) v_2 , using the concentration $c=0.5$ for A atom with the coordination number $z=4$.

(1), the average energy of the microstate in the Bragg Will-iams approximation is

$$\langle W \rangle = W_0 + \frac{1}{2}NzS^2v_1 + \frac{1}{2}NSv_2, \quad (5)$$

where

$$W_0 = \frac{Nz}{2} [c^2(2v_{AA}^{(1)} + v_{AA}^{(2)}) + (1-c)^2(2v_{BB}^{(1)} + v_{BB}^{(2)}) + 2c(1-c) \times (2v_{AB}^{(1)} + v_{AB}^{(2)})] + N[c(v_{A\alpha} + v_{A\beta}) + (1-c)(v_{B\alpha} + v_{B\beta})],$$

$$v_1 = \left[v_{AB}^{(1)} - \frac{1}{2}(v_{AA}^{(1)} + v_{BB}^{(1)}) \right] - \frac{1}{2} \left[v_{AB}^{(2)} - \frac{1}{2}(v_{AA}^{(2)} + v_{BB}^{(2)}) \right],$$

and

$$v_2 = (v_{A\alpha} - v_{A\beta}) + (v_{B\beta} - v_{B\alpha}).$$

z is the coordination number of the α or β sites. Usually, the order transition between the A and B atoms occurs regularly with a decrease in temperature if $v_1 < 0$, where v_2 is the energy difference of A and B atoms occupying α or β sites. It can predict which ones are the preferential occupancy sites for the A and B atoms, viz. α or β . The existence of a non-hydrostatic elastic field will break the degeneracy of the site energy of the α and β sublattices in the tetragonal phase of YBCO and cause a preferential occupancy of one sublattice at the expense of the other.

According to the fundamental formula of thermodynamics for the Helmholtz free energy, F , of the system, and assuming a random occupancy of the sites within a given sublattice, i.e., no pair correlations, we obtain

$$F(S) - F(0) = \frac{N}{2}kT \{ (2c+S)\ln(2c+S) + (2c-S)\ln(2c-S) + [2(1-c)+S]\ln[2(1-c)+S] + [2(1-c)-S]\ln[2(1-c)-S] \} + \frac{N}{2}zv_1S^2 + \frac{N}{2}v_2S. \quad (6)$$

The equilibrium value of S is obtained by minimizing the free energy, $F(S)$. Thus, the condition $\frac{\partial F(S)}{\partial S} = 0$ gives

$$\ln \frac{(2c-S)[2(1-c)-S]}{(2c+S)[2(1-c)+S]} = \frac{2zv_1S + v_2}{kT}. \quad (7)$$

By calculating a value of v_2 as a function of the components of the elastic field tensor, inserting in Eq. (7) together with a value of the temperature T and solving for S will yield in the Bragg-Williams (mean-field) approximation, then will yield up to three real roots for the equilibrium value of S . In the most general case, one root will be a stable equilibrium point, one will be an unstable equilibrium, and one will be a metastable equilibrium point. When v_1 is negative and v_2 is zero, there will exist a critical value of the temperature, T_c , below which there will be three real roots for S at each temperature (the long-range ordered state for which the absolute value of S is nonzero, a pair of degenerate values, one positive and one negative, which characterize a state of stable equilibrium long-range order, and one root with $S=0$ which corresponds to unstable equilibrium). This is illustrated in Fig. 2(b). For temperatures above T_c , there will be one real root at $S=0$, which corresponds to the oxygen-disordered tetragonal state of YBCO.

When a nonhydrostatic elastic strain gives rise to a non-zero value of v_2 , the degeneracy of the two ordered states is broken, one of the sublattices becomes energetically favored, and if the strain energy is not too large, the nonhydrostatic strain will form spontaneously. (This is just what happens for volumetric strains in the simplest models of the compressible Ising model of ferromagnetism.) This state corresponds to the orthorhombic state of YBCO.

At temperatures above T_c , the presence of the same non-hydrostatic strain will require an externally applied stress or the presence of an internal strain (intrinsically nonhomogeneous) caused by the presence structural defects such as dislocations. The effect of such a strain is to cause state of nonzero long-range order at equilibrium at temperatures where the long-range order parameter is zero in a strain-free system, illustrated in Fig. 3. This is effect is precisely analogous to the effect of a magnetic field on the magnetic moment of a paramagnetic materials. We can thus say that the elastic Bragg-Williams model of oxygen-order/disorder in YBCO exhibits paraelastic long-range order.

B. Bethe's theory

The mean-field Bragg-Williams method outlined above has the deficiency that it neglects the effects of short-range

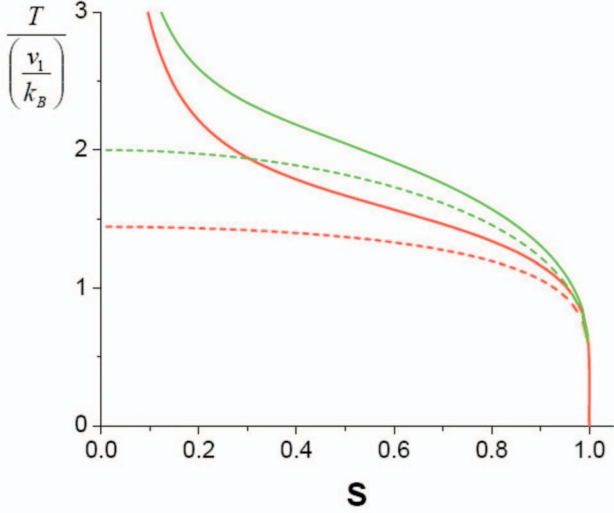


FIG. 3. (Color) The relationship between temperature and order parameter with $c=0.5$ and $z=4$. Green lines are Bragg-Williams approximation; red lines are Bethe approximation. Dotted lines are $v_2=0$; solid lines are $v_2=v_1/2$.

order, as characterized by the correlations in the type of species occupying various kinds of pairs of sites. In this study we considered two types of site pairs: those without and with a Cu atom between them, denoted by superscripts 1 and 2, respectively. We also will utilize the method proposed by Bethe² as implemented by Easthope³ to minimize the Helmholtz free energy with respect to the pair occupation probabilities.

In this section, we follow Easthope's method³ to study the relationship of the degree of order with temperature. When the central site is an α site, and is occupied by an A (oxygen) atom while n atoms in the nearest-neighbor shell are also A atoms, then the partition function for this configuration is

$$f_{A\alpha}^n = \lambda_{A\alpha} \lambda_{A\beta}^n \mu_{B\beta}^{z-n} \binom{z}{n} e^{-nv_{AA}^{(1)}/kT} e^{-(z-n)v_{AB}^{(1)}/kT} \varepsilon'^n. \quad (8a)$$

When the central site is occupied by a B atom (vacancy), it is

$$f_{B\alpha}^n = \lambda_{A\beta}^n \mu_{B\beta}^{z-n} \mu_{B\alpha} \binom{z}{n} e^{-nv_{AB}^{(1)}/kT} e^{-(z-n)v_{BB}^{(1)}/kT} \varepsilon'^n. \quad (8b)$$

The complete partition function for an α site corresponding to central atoms A or B is given by $f_{A\alpha} + f_{B\alpha}$, where

$$f_{A\alpha} = \sum_n f_{A\alpha}^n = \lambda_{A\alpha} (\lambda_{A\beta} e^{-v_{AA}^{(1)}/kT} \varepsilon' + \mu_{B\beta} e^{-v_{AB}^{(1)}/kT})^z, \quad (9a)$$

$$f_{B\alpha} = \sum_n f_{B\alpha}^n = \mu_{B\alpha} (\lambda_{A\beta} e^{-v_{AB}^{(1)}/kT} \varepsilon' + \mu_{B\beta} e^{-v_{BB}^{(1)}/kT})^z. \quad (9b)$$

Similar expressions can be obtained for a central β site

$$f_{A\beta} = \sum_n f_{A\beta}^n = \lambda_{A\beta} (\lambda_{A\alpha} e^{-v_{AA}^{(1)}/kT} + \mu_{B\alpha} e^{-v_{AB}^{(1)}/kT} \eta')^z, \quad (10a)$$

$$f_{B\beta} = \sum_n f_{B\beta}^n = \mu_{B\beta} (\lambda_{A\alpha} e^{-v_{AB}^{(1)}/kT} + \mu_{B\alpha} e^{-v_{BB}^{(1)}/kT} \eta')^z, \quad (10b)$$

where ε' and η' were introduced by Easthope³ to describe the case where the first shell consists of α sites, and one where it consists of β sites, respectively. We define $x = e^{v_1/kT} = e^{-(v_{AA}^{(1)} + v_{BB}^{(1)} - 2v_{AB}^{(1)})/2kT}$ (the interaction of nearest neighbors only is considered, because the precision in calculation is only slight improved when the interaction of next-nearest neighbor is considered²); $\kappa = e^{-(v_{AA}^{(1)} - v_{BB}^{(1)})/2kT}$; $\varepsilon = \frac{\lambda_{A\beta}}{\mu_{B\beta}} \kappa \varepsilon'$, and $\eta = \frac{\mu_{B\alpha}}{\lambda_{A\alpha} \kappa} \eta'$, then we can rewrite Eqs. (9) and (10) as follows:

$$f_{A\alpha} = \lambda_{A\alpha} (\varepsilon x + 1)^z \mu_{B\beta}^z e^{-zv_{AB}^{(1)}/kT}, \quad (11a)$$

$$f_{B\alpha} = \mu_{B\alpha} (\varepsilon + x)^z \left(\frac{\mu_{B\beta}}{\kappa} \right)^z e^{-zv_{AB}^{(1)}/kT}, \quad (11b)$$

$$f_{A\beta} = \lambda_{A\beta} (x + \eta)^z (\kappa \lambda_{A\alpha})^z e^{-zv_{AB}^{(1)}/kT}, \quad (11c)$$

$$f_{B\beta} = \mu_{B\beta} (1 + \eta x)^z \lambda_{A\alpha}^z e^{-zv_{AB}^{(1)}/kT}. \quad (11d)$$

The fraction of A and B atoms occupying an α or β site can be calculated, respectively, by

$$c_{A\alpha} = \frac{f_{A\alpha}}{f_{A\alpha} + f_{B\alpha}}, \quad (12a)$$

$$c_{A\beta} = \frac{f_{A\beta}}{f_{A\beta} + f_{B\beta}}, \quad (12b)$$

$$c_{B\alpha} = \frac{f_{B\alpha}}{f_{A\alpha} + f_{B\alpha}}, \quad (12c)$$

$$c_{B\beta} = \frac{f_{B\beta}}{f_{A\beta} + f_{B\beta}}. \quad (12d)$$

The fraction of A atoms on β sites regarded as central sites occupied by A atoms should be equal to the fraction of A atoms in the first shell sites surrounding any α site;

$$\begin{aligned} c_{A\beta} &= \frac{1}{z} \frac{\sum_n n (f_{A\alpha}^n + f_{B\alpha}^n)}{f_{A\alpha} + f_{B\alpha}} \\ &= \frac{\varepsilon}{z} \frac{\partial \ln(f_{A\alpha} + f_{B\alpha})}{\partial \varepsilon} \\ &= \frac{\varepsilon x}{1 + \varepsilon x} c_{A\alpha} + \frac{\varepsilon}{\varepsilon + x} c_{B\alpha}. \end{aligned} \quad (13a)$$

Similarly, by considering the fraction of B atoms occupying the α sites, we have

$$\begin{aligned}
c_{B\alpha} &= \frac{1}{z} \frac{\sum_n n(f_{A\beta}^n + f_{B\beta}^n)}{f_{A\beta} + f_{B\beta}} \\
&= \frac{\eta}{z} \frac{\partial \ln(f_{A\beta} + f_{B\beta})}{\partial \eta} \\
&= \frac{\eta x}{1 + \eta x} c_{B\beta} + \frac{\eta}{\eta + x} c_{A\beta}. \quad (13b)
\end{aligned}$$

If c is the concentration of the A atoms, then, according to the definition of the degree of order in Eq. (2), we have

$$c_{A\alpha} = \frac{1}{2}(S + 2c), \quad (14a)$$

$$c_{A\beta} = \frac{1}{2}(2c - S), \quad (14b)$$

$$c_{B\beta} = 1 - \frac{1}{2}(2c - S), \quad (14c)$$

$$c_{B\alpha} = 1 - \frac{1}{2}(S + 2c). \quad (14d)$$

Substituting Eq. (14) into Eq. (13) leads to

$$\frac{1}{2}(2c - S) = \frac{1}{2} \frac{\varepsilon x}{1 + \varepsilon x} (S + 2c) + \frac{\varepsilon}{\varepsilon + x} \left[1 - \frac{1}{2}(S + 2c) \right], \quad (15a)$$

$$1 - \frac{1}{2}(S + 2c) = \frac{\eta x}{1 + \eta x} \left[1 - \frac{1}{2}(2c - S) \right] + \frac{1}{2} \frac{\eta}{\eta + x} (2c - S). \quad (15b)$$

The values of ε and η can be determined as function of S from Eq. (15). We also can obtain from expressions $c_{B\alpha}/c_{A\alpha} = f_{B\alpha}/f_{A\alpha}$ and $c_{A\beta}/c_{B\beta} = f_{A\beta}/f_{B\beta}$

$$\begin{aligned}
\frac{(2c - S) \left[1 - \frac{1}{2}(2c + S) \right]}{(2c + S) \left[1 - \frac{1}{2}(2c - S) \right]} &= \frac{\lambda_{A\beta} \mu_{B\alpha}}{\lambda_{A\alpha} \mu_{B\beta}} \frac{(\varepsilon + x)^z (\eta + x)^z}{(\varepsilon x + 1)^z (\eta x + 1)^z}. \quad (16)
\end{aligned}$$

The difference between Eq. (16) and Easthope's result is the appearance of the term $\frac{\lambda_{A\beta} \mu_{B\alpha}}{\lambda_{A\alpha} \mu_{B\beta}}$ in the right side of Eq. (16). Because $\lambda_{A\alpha}$, $\lambda_{A\beta}$, $\mu_{B\alpha}$, and $\mu_{B\beta}$ have $\lambda_{A\alpha} \propto e^{-v_{A\alpha}/kT}$, $\lambda_{A\beta} \propto e^{-v_{A\beta}/kT}$, $\mu_{B\alpha} \propto e^{-v_{B\alpha}/kT}$, and $\mu_{B\beta} \propto e^{-v_{B\beta}/kT}$, we get

$$\frac{\lambda_{A\beta} \mu_{B\alpha}}{\lambda_{A\alpha} \mu_{B\beta}} = e^{[(v_{A\alpha} - v_{A\beta}) + (v_{B\beta} - v_{B\alpha})]/kT} = e^{v_2/kT}. \quad (17)$$

Combining Eqs. (15a), (15b), (16), and (17), we can obtain the degree of long-range order S as a function of x , which also is a function of temperature.

III. RESULTS AND DISCUSSION OF THE CALCULATION OF LONG-RANGE ORDER IN INTERNALLY STRAINED YBCO

Using above formulae, we can calculate the relationship between free energy, order parameter, and temperature. Equation (6) is similar to the mean-field theory of magnetic phase transitions within an external magnetic field when the latter is replaced by v_2 (Ref. 20), where v_2 is defined following Eq. (5), and has a nonzero value in the presence of a nonhydrostatic elastic strain. The symmetry of free energy $F(S) = F(-S)$ is broken due to v_2 's existence (Fig. 2). The minimum point of free energy is not at $S=0$, even at high temperature [Fig. 2(a)]. This means that the long-range order does not vanish at any finite temperature. At temperatures below the order-disorder phase transition, there is only one stable order state, and the other becomes metastable [Fig. 2(b)]. Figure 3, illustrating the relationship between temperature and the degree of long-range order, S , in the stable state, indicates clearly that S does not disappear at finite temperature when v_2 is not zero. From Figs. 2 and 3, we see that there are two main differences from the usual strain-free order-disorder theory when the *a priori* probabilities of atoms occupying ordering sites are different, i.e., v_2 is not zero: (1) the formation probability, Figs. 1(b) and 1(c), differs and (2) long-range order may exist at high temperature.

The oxygen disorder-order transition in the Cu-O plane of $\text{YBa}_2\text{Cu}_3\text{O}_{6+x}$ is accompanied by a change in lattice structure from tetragonal to orthorhombic caused by the spontaneous formation of a nonhydrostatic strain during cooling, even in the absence of applied stress or internal stress from defects. This transition can produce two equivalent variants [Figs. 1(b) and 1(c)] connected by [110] twinning. In the orthorhombic phase, the b lattice elongates and the a lattice contracts compared with the tetragonal phase. The ordering process is such that most oxygen atoms in Cu-O plane are localized to $(0\frac{1}{2}0)$ sites along the b axis. If stress fields cause the elongation of lattice of the tetragonal phase along the y axis (the [010] direction) and contraction along the x axis (the [100] direction), the formation energy of oxygen atoms occupying α sites will differ from that for the β sites, therefore, the probability of oxygen atoms occupying these sites will be different too [Fig. 1(d)]. In that situation, oxygen atoms will preferentially occupy α site along the y axis [Fig. 1(b)]; conversely, oxygen atoms will advantageously occupy β site along the x axis [Fig. 1(c)].

The theory of thermochemical equilibrium of solid under stress was discussed extensively by Larché and Cahn.²¹ Their theory indicates that the action of stress will change the chemical potential of an interstitial atom in an elastically strained matrix. Utilizing this theory, an expression for the stress dependence of the parameter v_2 , introduced in Sec. II above, can be obtained under stress. It is

$$v_2 = - \frac{\partial \varepsilon_{ij}^c}{\partial c_{A\alpha}} \sigma_{ij} - \frac{\partial \varepsilon_{ij}^c}{\partial c_{A\beta}} \sigma_{ij}, \quad (18)$$

where ε_{ij}^c is the strain due to a change in oxygen concentration occupying α and β sites; σ_{ij} is the net stress arising from

external sources and from defects in the lattice. Combining Eqs. (14a), (14b), and (18), we have

$$v_2 = -2 \left(\frac{\partial \varepsilon_{xx}^c}{\partial S} \sigma_{xx} - \frac{\partial \varepsilon_{yy}^c}{\partial S} \sigma_{yy} \right). \quad (19)$$

Next, we apply our theory to discuss the change in the degree of oxygen order in the stress field around a dislocation, near a twin tip, and to explain some experimental phenomena. Let us now consider the effect on the degree of order of the presence of an edge dislocation in $\text{YBa}_2\text{Cu}_3\text{O}_{6+x}$, with a Burgers vector $\mathbf{b}=[010]$ and a dislocation line in the (100) plane.²² The dislocation produces stress components σ_{xx} and σ_{yy} (Ref. 23),

$$\sigma_{xx} = \frac{K_1 b x (x^2 - \lambda^2 y^2)}{2\pi (x^4 - 2\lambda x^2 y^2 + \lambda^4 y^4)}, \quad (20a)$$

$$\sigma_{yy} = \frac{K_2 b x [x^2 + (\lambda^2 - 2\lambda) y^2]}{2\pi (x^4 - 2\lambda x^2 y^2 + \lambda^4 y^4)}, \quad (20b)$$

where $\lambda^2 = -\sqrt{\frac{c_{11}}{c_{22}}}$, $2\lambda = \frac{c_{12}^2 + 2c_{66}c_{12} - c_{11}c_{22}}{c_{66}c_{22}}$, $K_1 = \frac{s_{33}}{(s_{11}s_{33} - s_{31}^2)\sqrt{2(\lambda^2 - \lambda)}}$, and $K_2 = \frac{K_1}{\lambda^2}$. c_{11} and s_{11} , etc. are respectively stiffness and compliance coefficients.

Using the lattice parameters for $\text{YBa}_2\text{Cu}_3\text{O}_7$ obtained in Ref. 24, $a=3.822$ Å, $b=3.891$ Å, $c=11.677$ Å, and $a_t \approx \frac{a+b}{2} = 3.856$ Å, and assuming the degree of order is perfect, i.e., $S=1$, when these values of the lattice parameters of the orthorhombic phase in Ref. 24 are used, we have

$$\frac{\partial \varepsilon_{xx}^c}{\partial S} = -0.009,$$

$$\frac{\partial \varepsilon_{yy}^c}{\partial S} = 0.009,$$

and unit-cell volume

$$V = 173 \text{ \AA}^3.$$

The elastic constants of the orthorhombic phase are $c_{11}=231$ GPa, $c_{22}=268$, $c_{33}=186$, $c_{44}=49$, $c_{55}=37$, $c_{66}=95$, $c_{12}=132$, $c_{13}=71$, and $c_{23}=95$ from Ref. 25. The elastic constants of the tetragonal phase used in our calculation are approximated as $c_{11}=c_{22}=\frac{1}{2}(231+268) \approx 250$ GPa, $c_{12}=c_{13}=83$, $c_{44}=c_{55}=37$, and others the same as those of the orthorhombic phase. v_2 can be calculated from Eqs. (19) and (20). Using the oxygen interaction data given by Semenovskaya and Khachatryan,²⁶ we obtain $v_1 = -638 \times 10^{-23}$ J and an ordering temperature of 924 K when v_2 is zero. Figure 4 shows our calculated results for the long-range order parameter S in the vicinity of the edge dislocation. In this calculation we have ignored the presence of gradient terms in the free energy of order disorder, such as those in the Cahn-Hilliard theory of nonhomogeneous order.²¹ The figure shows the degree of long-range order in the lattice around an edge dislocation with Burgers vector $\mathbf{b}=[010]$ with oxygen concentration $x=1$ at temperature, 1000 K, which is above the stress-free critical ordering temperature, thus the degree of long-range order far from the dislocation is zero. The

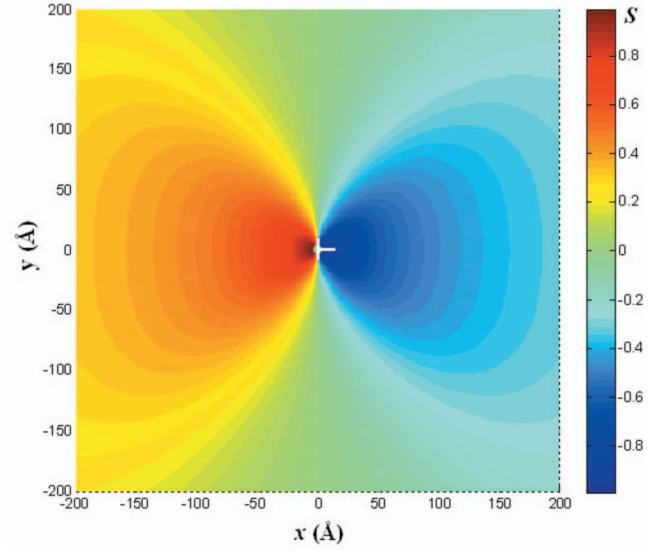


FIG. 4. (Color) The change of oxygen ordering degree around an edge dislocation or $\mathbf{b}=[010]$ with $\delta=1$ and $T=1000$ K. It is more than normal critical $T_c=924$ K.

orientation of oxygen ordering reverses on opposite sides of the dislocation glide plane, i.e., if oxygen atoms on one side of the glide plane preferentially occupy α sites [Fig. 1(b)], then on the other side oxygen prefers β sites [Fig. 1(c)]. The spatially inhomogeneous enhancement of long-range order means that upon cooling from the disordered tetragonal phase, nuclei of orthorhombic phase are producing first near the dislocation. When the perfect lattice dislocation with Burgers vector $[010]$ dissociates $[010] \rightarrow \frac{1}{2}[\bar{1}10] + \frac{1}{2}[110]$, the dislocations with Burgers vectors $\frac{1}{2}[\bar{1}10]$ and $\frac{1}{2}[110]$ may then become twinning dislocations in the orthorhombic phase of $\text{YBa}_2\text{Cu}_3\text{O}_{6+x}$ (Ref. 27). Zhu *et al.*'s experiment²⁸ confirmed that the two kinds of twinning dislocations $\frac{1}{2}[\bar{1}10]$ and $\frac{1}{2}[110]$ frequently are encountered within one crystal grain in $\text{YBa}_2\text{Cu}_3\text{O}_{6+x}$.

The shape of a lenticular twin in orthorhombic YBCO can be quantitatively described as a simple geometrical corollary by using a dislocation model based on the mechanical equilibrium distribution of twinning dislocations in a double pile-up.²⁸⁻³⁰ At the twin tip, the dislocation density and the thickness functions are³⁰

$$\rho(x) = \frac{4M(1-\nu)}{\mu b \sqrt{L}} \frac{x}{\sqrt{L^2 - x^2}}, \quad (21)$$

$$y(x) = \frac{4dM(1-\nu)}{\mu b \sqrt{L}} \sqrt{L^2 - x^2}, \quad (22)$$

where M is a constant; μ and ν are the shear modulus and Poisson's ratio, respectively; b is the magnitude of the dislocation Burgers vector, d is the interplanar distance of the glide planes of twinning dislocations, and L is the length of the twin tip. The total stress σ_{ij}^{tot} on the region of the twin tip can be calculated by a line integral:

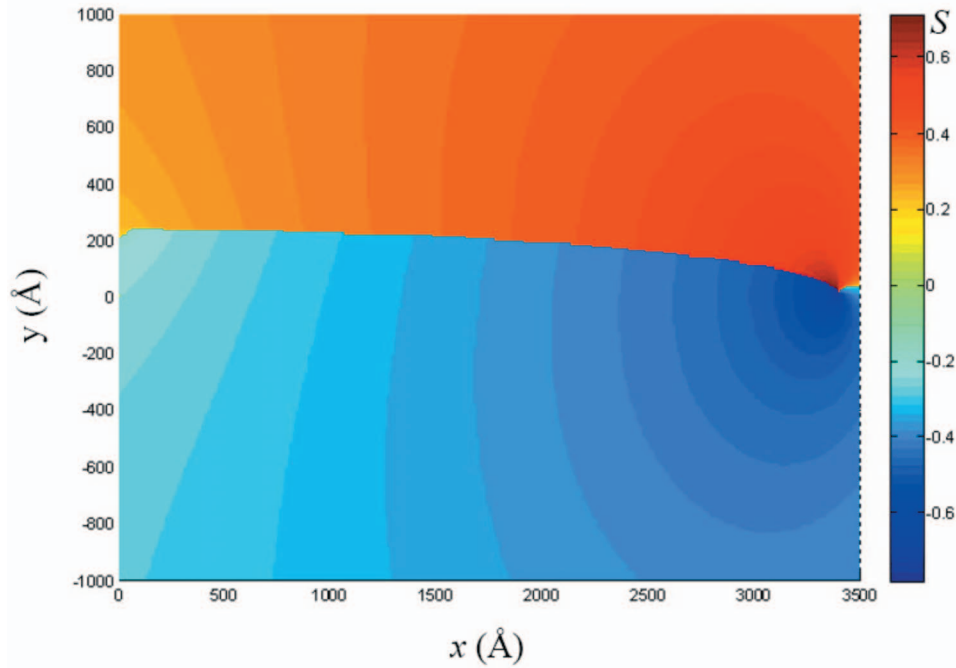


FIG. 5. (Color) The change of oxygen ordering degree near twin tip at temperature 910 K.

$$\sigma_{ij}^{\text{tot}} = \int_0^L \rho(x') \sigma_{ij}(\mathbf{r} - \mathbf{r}') \sqrt{1 + \left(\frac{dy(x')}{dx'}\right)^2} dx'. \quad (23)$$

An approximation of elastic isotropy is assumed in this calculation. $\sigma_{ij}(\mathbf{r} - \mathbf{r}')$ is the stress of a dislocation at position \mathbf{r}' , and explicit expressions are given by Hirth and Lothe.²⁹ Using $M = 5.01 \times 10^4 \text{ N/m}^{3/2}$, $L = 3400 \text{ \AA}$,³⁰ $\mu = c_{66} = 95 \text{ GPa}$, $\nu = 0.314$,²⁵ Burgers vector \mathbf{b} of edge twinning dislocation as $\mathbf{b} = |b - a|[110]$,^{27,28} i.e., $|\mathbf{b}| = 0.098 \text{ \AA}$, and $d = d_{110} = 2.726 \text{ \AA}$, the stress components near the twin tip are calculated numerically with Eqs. (21)–(23). Because the orientation of the Burgers vector of a twinning dislocation is $[110]$, a coordinate conversion should be done when we calculate ν_2 using Eq. (19). Finally, the degree of the oxygen ordering in the region of the twin tip is obtained from Eq. (7). Figure 5 is the calculated result and shows the change of oxygen ordering in the region of the twin tip.

The theories of order-disorder phase transition indicate that the degree of long-range order depends significantly on the temperature and rapidly reaches its limit with the decrease in temperature below the critical temperature T_c . A small change in the value of ν_2 in our theory will bring on a drastic change in the degree of order degree T_c . Figures 4 and 5 demonstrate this change, suggesting the large effect of crystal defects on oxygen ordering, especially when temperature is near T_c . $\text{YBa}_2\text{Cu}_3\text{O}_{6+x}$ often exhibits regions of structural inhomogeneity.^{31–34} These inhomogeneities may come from the local change in oxygen concentration and the degree of oxygen ordering, as well as the presence of different phases related to oxygen ordering. The vapor pressure of oxygen in the environment of a crystal determines the chemical potential of oxygen and consequently determines the equilibrium oxygen concentration in $\text{YBa}_2\text{Cu}_3\text{O}_{6+x}$.^{18,35,36} The oxygen-ordering phases,^{16,19} such as OI ($x=1$), OII ($x=0.5$), OIII ($x=0.67$), etc., in $\text{YBa}_2\text{Cu}_3\text{O}_{6+x}$, are controlled

by the local oxygen concentration. Johnson *et al.*'s experiments³⁴ prove these ordering phases yield structural inhomogeneities and break the twin symmetry. Our study indicates that the local strain due to crystal defects also can cause structural inhomogeneities. Sarikaya and Stern's experiment³¹ found the structural variations in region of twin tip. A possible explanation is the action of twinning dislocation.

Applied stresses might also change the transition temperature of superconductivity in $\text{YBa}_2\text{Cu}_3\text{O}_{6+x}$ and similar materials.^{37–49} The effects of applied stress on single crystals or textured polycrystals will be anisotropic. The transition temperature of superconductivity increases with increased pressure along the b and c axes, but decreases with pressure along the a axis, as supported by some theoretical calculations.^{50–53} The microscopic origin of the resulting action usually is considered as pressure-induced charge rearrangements in the CuO_2 plane.^{50–56} The stress-induced change in the a and b axes would affect the degree of oxygen ordering of the orthorhombic structure;⁴⁰ for example, the b axis is shortened with more oxygen ordering in the orthorhombic $\text{YBa}_2\text{Cu}_3\text{O}_{6.41}$.⁵⁷ High-resolution thermal expansion measurements revealed that a glasslike transition occurs in $\text{YBa}_2\text{Cu}_3\text{O}_{6.95}$ related to oxygen ordering near room temperature,⁵⁸ and this glasslike transition reflects the contraction of the b and c axes, and the expansion of the a axis. These experimental and theoretical results signify that the contraction of the b axis of the orthorhombic phase increases the degree of oxygen ordering near room temperature, with the inverse result for the a axis. We believe that the origin of these ordering processes with b -axis compression and the glasslike transition is associated with the *a priori* probability of oxygen-occupied α or β sites in the Cu-O plane because of the inequivalence of the α and β sites in the orthorhombic structure, i.e., $\nu_2 \neq 0$. Therefore, the change of oxygen ordering from the pressure-induced or glasslike transition in the

orthorhombic phase can be considered as the transition from the A point on the solid line to the C point on the dash line, or from the B point on the solid line to the D point on the dash-dotted one in Fig. 2(b). This transition is from one

orthorhombic structure to another, where the change in the degree of oxygen ordering is subtle, but the change in free energy is evident. The free energy of this transition can be written as

$$F(S) = \begin{cases} \frac{N}{2}kT\{(2c + S_1)\ln(2c + S_1) + (2c - S_1)\ln(2c - S_1) + [2(1 - c) + S_1]\ln[2(1 - c) + S_1] + [2(1 - c) - S_1]\ln[2(1 - c) - S_1]\} \\ + \frac{N}{2}zv_1S_1^2 & \text{for } T > T'_c \\ \frac{N}{2}kT\{(2c + S_2)\ln(2c + S_2) + (2c - S_2)\ln(2c - S_2) + [2(1 - c) + S_2]\ln[2(1 - c) + S_2] + [2(1 - c) - S_2]\ln[2(1 - c) - S_2]\} \\ + \frac{N}{2}zv_1S_2^2 + \frac{N}{2}v_2S_2 & \text{for } T < T'_c, \end{cases}$$

where T'_c is the temperature of the phase transition, and S_1 and S_2 are the long-range order parameters before and after the transition. After this transition, the oxygen atoms in the CuO plane are more likely to occupy the b axis, and the degree of oxygen ordering will be larger than before.

Epitaxial films often exhibit strain due to lattice mismatch between the film and the substrate, yielding differences in structure and properties, as reported for $\text{YBa}_2\text{Cu}_3\text{O}_{6+x}$ films with various substrates.^{59,60} This may well be explained by the associated lattice mismatch strain-induced oxygen ordering as discussed above.

IV. CONCLUSIONS

The changes in lattice symmetry and interatomic bond lengths of an oxide due to stress or crystalline defects can be accompanied by a change in the symmetry of the occupied sites of ordering atoms. Accordingly, the thermodynamics of the order-disorder transition in superconducting perovskites will be altered. Modifications of the order-disorder theories of Bragg-Williams and Bethe to include the effects of internal elastic strain caused by defects or applied stresses show

that this change will establish long-range order at any finite temperature and will change the state of order below the transition temperature compared to that of a strain-free crystal. Applying these modified theories of the thermodynamics to $\text{YBa}_2\text{Cu}_3\text{O}_{6+x}$, the oxygen-ordering domains near an edge dislocation in crystal of $\text{YBa}_2\text{Cu}_3\text{O}_{6+x}$ were calculated for temperatures above that of the strain-free and the tetragonal-to-orthorhombic transformations; the stress-induced oxygen-ordering domains formed in the tetragonal phase may be the nuclei of the orthorhombic phase when this phase transformation is triggered by a decrease in temperature. The twinning dislocations in a twin tip can result in structural inhomogeneity. In the orthorhombic phase, the effect of stress in different directions or charge rearrangements in the CuO_2 plane modifies the oxygen ordering process, thus changing the superconducting transition temperature.

ACKNOWLEDGMENTS

The work was supported by U.S. Department of Energy, Office of Basic Energy Science, under Contract No. DE-AC02-98CH10886.

*zhu@bnl.gov

¹W. L. Bragg and E. J. Williams, Proc. R. Soc. London, Ser. A **145**, 699 (1934); E. J. Williams, *ibid.* **152**, 231 (1935).

²H. A. Bethe, Proc. R. Soc. London, Ser. A **150**, 552 (1935).

³C. E. Easthope, Proc. Camb. Philos. Soc. **33**, 502 (1937).

⁴J. G. Kirkwood, J. Chem. Phys. **6**, 70 (1938).

⁵R. H. Fowler and E. A. Guggenheim, Proc. R. Soc. London, Ser. A **174**, 189 (1940).

⁶T. Muto and Y. Takagi, in *Solid State Physics*, edited by R. Seitz and D. Turnbull (Academic, New York, 1955), Vol. 1, p. 193.

⁷R. Kikuchi, Phys. Rev. **81**, 988 (1951).

⁸L. Onsager, Phys. Rev. **65**, 117 (1944).

⁹Z. X. Cai and Y. Zhu, *Microstructures and Structural Defects in High-Temperature Superconductors* (World Scientific, Singapore, 1998).

¹⁰E. Dagotto, T. Hotta, and A. Moreo, Phys. Rep. **344**, 1 (2001).

¹¹R. Beyers, B. T. Ahn, G. Gorman, V. Y. Lee, S. S. P. Parkin, M. L. Ramires, K. P. Roche, J. E. Vazques, T. M. Gür, and R. A. Huggins, Nature (London) **340**, 619 (1989).

¹²B. W. Veal, H. You, A. P. Paulikas, H. Shi, Y. Fang, and J. W. Downey, Phys. Rev. B **42**, 4770 (1990); B. W. Veal, A. P. Paulikas, Hoydoo You, Hao Shi, Y. Fang, and J. W. Downey, *ibid.*

- 42**, 6305 (1990).
- ¹³A. Hosseini, D. M. Broun, D. E. Sheehy, T. P. Davis, M. Franz, W. N. Hardy, R. Liang, and D. A. Bonn, *Phys. Rev. Lett.* **93**, 107003 (2004).
- ¹⁴T. J. Sato, J. W. Lynn, and B. Dabrowski, *Phys. Rev. Lett.* **93**, 267204 (2004).
- ¹⁵O. Chmaissem, B. Dabrowski, S. Kolesnik, J. Mais, J. D. Jorgensen, S. Short, C. E. Botez, and P. W. Stephens, *Phys. Rev. B* **72**, 104426 (2005).
- ¹⁶A. G. Khachatryan and J. W. Morris, *Phys. Rev. Lett.* **61**, 215 (1988); A. G. Khachatryan, S. V. Semenovskaya, and J. W. Morris, Jr., *Phys. Rev. B* **37**, 2243 (1988).
- ¹⁷H. Shaked, J. D. Jorgensen, J. Faber, Jr., D. G. Hinks, and B. Dabrowski, *Phys. Rev. B* **39**, 7363 (1989).
- ¹⁸H. Bakker, D. O. Welch, and O. W. Lazareth, Jr., *Solid State Commun.* **64**, 237 (1987); H. Bakker, J. P. A. Westerveld, D. M. R. Locascio, and D. O. Welch, *Physica C* **157**, 25 (1989).
- ¹⁹L. T. Wille, *Phys. Rev. B* **40**, 6931 (1989); A. Berera and D. de Fontaine, *ibid.* **39**, 6727 (1989); L. T. Wille and D. de Fontaine, *ibid.* **37**, 2227 (1988); L. T. Wille, A. Berera, and D. de Fontaine, *Phys. Rev. Lett.* **60**, 1065 (1988); D. de Fontaine, L. T. Wille, and S. C. Moss, *Phys. Rev. B* **36**, 5709 (1987).
- ²⁰H. E. Stanley, *Introduction to Phase Transition and Critical Phenomena* (Oxford University Press, Oxford, 1971), p. 79.
- ²¹F. Larché and J. W. Cahn, *Acta Metall.* **21**, 1051 (1973); **26**, 53 (1976).
- ²²M. Verwerft, D. K. Dijken, J. T. M. De Hosson, and A. C. Van Der Steen, *Phys. Rev. B* **50**, 3271 (1994).
- ²³J. W. Steeds, *Introduction to Anisotropic Elasticity Theory of Dislocations* (Clarendon Press, Oxford, 1973), p. 44.
- ²⁴R. J. Cava, B. Batlogg, C. H. Chen, E. A. Rietman, S. M. Zahurak, and D. Werder, *Nature (London)* **329**, 423 (1987).
- ²⁵M. Lei, J. L. Sarrao, W. M. Visscher, T. M. Bell, J. D. Thompson, A. Migliori, U. W. Welp, and B. W. Veal, *Phys. Rev. B* **47**, 6154 (1993).
- ²⁶S. Semenovskaya and A. G. Khachatryan, *Phys. Rev. Lett.* **67**, 2223 (1991); *Phys. Rev. B* **46**, 6511 (1992).
- ²⁷Y. Zhu and M. Suenaga, *Philos. Mag. A* **66**, 457 (1992).
- ²⁸Y. Zhu, M. Suenaga, and J. Taftø, *Philos. Mag. A* **67**, 1057 (1993).
- ²⁹J. P. Hirth and J. H. Lothe, *Theory of Dislocations* (Wiley-Interscience, New York, 1982).
- ³⁰V. S. Boyko, Siu-Wai Chan, and M. Chopra, *Phys. Rev. B* **63**, 224521 (2001).
- ³¹M. Sarikaya and E. A. Stern, *Phys. Rev. B* **37**, 9373 (1988).
- ³²G. P. E. M. van Bakel, P. A. Hof, J. P. M. van Engelen, P. M. Bronsveld, and J. Th. M. De Hosson, *Phys. Rev. B* **41**, 9502 (1990).
- ³³T. Pereg-Barnea, P. J. Turner, R. Harris, G. K. Mullins, J. S. Bobowski, M. Raudsepp, R. Liang, D. A. Bonn, and W. N. Hardy, *Phys. Rev. B* **69**, 184513 (2004).
- ³⁴C. L. Johnson, J. K. Bording, and Y. Zhu, *Phys. Rev. B* **78**, 014517 (2008).
- ³⁵J. D. Jorgensen, B. W. Veal, A. P. Paulikas, L. J. Nowicki, G. W. Crabtree, H. Claus, and W. K. Kwok, *Phys. Rev. B* **41**, 1863 (1990).
- ³⁶P. Schleger, W. N. Hardy, and B. X. Wang, *Physica C* **176**, 261 (1991).
- ³⁷L. M. Ferreira, P. Pureur, H. A. Borges, and P. Lejay, *Phys. Rev. B* **69**, 212505 (2004).
- ³⁸L. X. Cao, R. K. Kremer, Y. L. Qin, J. Brotz, J. S. Liu, and J. Zegenhagen, *Phys. Rev. B* **66**, 054511 (2002).
- ³⁹X. J. Chen, H. Q. Lin, W. G. Yin, C. D. Gong, and H.-U. Haberman, *Phys. Rev. B* **64**, 212501 (2001).
- ⁴⁰S. Sadewasser, Y. Wang, J. S. Schilling, H. Zhang, A. P. Paulikas, and B. W. Veal, *Phys. Rev. B* **56**, 14168 (1997).
- ⁴¹R. P. Gupta and M. Gupta, *Phys. Rev. B* **50**, 9615 (1994).
- ⁴²S. L. Bud'ko, J. Guimpel, O. Nakamura, M. B. Maple, and I. K. Schuller, *Phys. Rev. B* **46**, 1257 (1992).
- ⁴³U. Welp, M. Grimsditch, S. Fleshler, W. Nessler, J. Downey, G. W. Crabtree, and J. Guimpel, *Phys. Rev. Lett.* **69**, 2130 (1992).
- ⁴⁴C. Meingast, O. Krauf, T. Wolf, H. Wuhl, A. Erb, and G. Müller-Vogt, *Phys. Rev. Lett.* **67**, 1634 (1991).
- ⁴⁵C. Meingast, B. Blank, H. Burkle, B. Obst, T. Wolf, H. Wuhl, V. Selvamanickam, and K. Salama, *Phys. Rev. B* **41**, 11299 (1990).
- ⁴⁶M. F. Crommie, A. Y. Liu, A. Zettl, M. L. Cohen, P. Parilla, M. F. Hundley, W. N. Creager, S. Hoen, and M. S. Sherwin, *Phys. Rev. B* **39**, 4231 (1989).
- ⁴⁷H. A. Borges, R. Kwok, J. D. Thompson, G. L. Wells, J. L. Smith, Z. Fisk, and D. E. Peterson, *Phys. Rev. B* **36**, 2404 (1987).
- ⁴⁸A. Driessen, R. Griessen, N. Koeman, E. Salomons, R. Brouwer, D. G. de Groot, K. Heeck, H. Hemmes, and J. Rector, *Phys. Rev. B* **36**, 5602 (1987).
- ⁴⁹J. E. Schirber, D. S. Ginley, E. L. Venturini, and B. Morosin, *Phys. Rev. B* **35**, 8709 (1987).
- ⁵⁰W. E. Pickett, *Phys. Rev. Lett.* **78**, 1960 (1997).
- ⁵¹M. W. Klein and S. B. Simanovsky, *Phys. Rev. Lett.* **78**, 3927 (1997).
- ⁵²A. Perali and G. Varelogiannis, *Phys. Rev. B* **61**, 3672 (2000).
- ⁵³X. J. Chen, H. Q. Lin, W. G. Yin, C. D. Gong, and H.-U. Haberman, *Phys. Rev. B* **64**, 212501 (2001).
- ⁵⁴I. D. Brown, *J. Solid State Chem.* **82**, 122 (1989); *J. Solid State Chem.* **90**, 155 (1991).
- ⁵⁵J. D. Jorgensen, S. Pei, P. Lightfoot, D. G. Hinks, B. W. Veal, B. Dabrowski, A. P. Paulikas, R. Kleb, and I. D. Brown, *Physica C* **171**, 93 (1990).
- ⁵⁶A. A. Aligia and J. Garcés, *Phys. Rev. B* **49**, 524 (1994).
- ⁵⁷J. D. Jorgensen, S. Pei, P. Lightfoot, H. Shi, A. P. Paulikas, and B. W. Veal, *Physica C* **167**, 571 (1990).
- ⁵⁸P. Nagel, V. Pasler, C. Meingast, A. I. Rykov, and S. Tajima, *Phys. Rev. Lett.* **85**, 2376 (2000).
- ⁵⁹R. Wördenweber, *Supercond. Sci. Technol.* **12**, R86 (1999).
- ⁶⁰G. L. Belenky, S. M. Green, A. Roytburd, C. J. Lobb, S. J. Hagen, R. L. Greene, M. G. Forrester, and J. Talvacchio, *Phys. Rev. B* **44**, 10117 (1991).